Ruthenium-catalyzed deformylative C–C activation and carbene insertion towards diversity-oriented synthesis of unsymmetrical biaryldiols and heterobiaryl amino alcohols

Chandan Kumar Giri[a], Tejender Singh[b†], Sudeshna Mondal[a†], Soumya Ghosh*[b] and Mahiuddin Baidya*[a]

[a]Department of Chemistry, Indian Institute of Technology Madras, Chennai 600036, India.

[b]Tata Institute of Fundamental Research (TIFR), Hyderabad, Telangana 500046, India.

[†]These authors contributed equally to this work.

Keywords: Ruthenium Catalysis, C–C Activation, Deformylation, Diazocarbenes, Unsymmetrical Biaryldiols, DFT study.

Abstract:

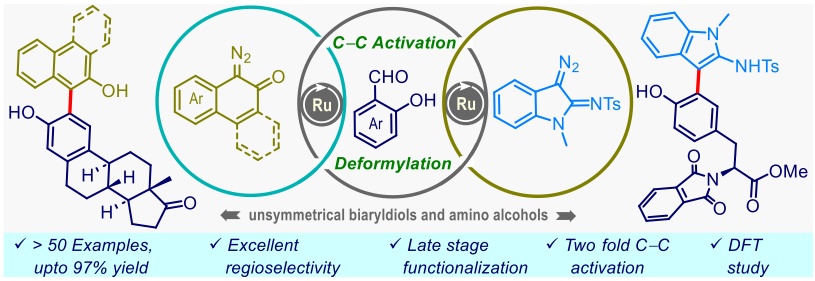

While 1,1′-biaryl diols and amino alcohols are privileged scaffolds, their streamlined catalytic synthesis with unsymmetrical substitution patterns remains a daunting challenge. Herein, we describe the first ruthenium(II)-catalyzed synthesis of unsymmetrical 1,1′-biaryl-2,2′-diols via a deformylative coupling of *ortho*-hydroxy aromatic aldehydes with diverse cyclic diazo compounds. The protocol is operationally simple, scalable, and involves intriguing C–C bond activation and carbene insertion cascade to produce a range of diversely functionalized biaryl diols in very high to excellent yields and regioselectivity. The methodology is also suitable to access heterobiaryl amino alcohols bearing indole motif, applicable in challenging two-fold C–C activation leading to valuable tetrahydroxy bis-biaryls, and retains efficacy in the site-selective modification of pharmaceutical agents. DFT studies have also been conducted to illustrate the intricacy of this catalytic cycle.

INTRODUCTION

Biaryl molecules, particularly biaryldiols, are prevalent in diverse natural products and bioactive compounds, and serve as pivotal backbones in designing valuable ligands and catalysts (Scheme 1a).[1,2] They are also high-value synthons for the production of sophisticated functional materials.[1c–d] Consequently, catalytic synthesis and facile diversification of biaryldiols have perennially intrigued the synthetic community. In this context, biaryldiols with symmetrical substitution patterns are within reach through a number of synthetic procedures; however, harnessing unsymmetrical biaryldiol frameworks poses an increasingly challenging task.[2] The transition-metal catalyzed cross-coupling reactions that have revolutionized the synthesis of biaryl scaffolds cannot be directly adopted for this purpose as they necessitate the utilization of suitably adorned prefunctionalized substrates and also, the presence of a phenolic hydroxyl group introduces intricacies that impede catalytic efficiency in a complex setting. Thus, engineering catalytic modular strategies to streamline the diversity-oriented construction of unsymmetrical biaryldiol molecular architectures from readily available starting materials would greatly enrich the synthetic chemist's repertoire.

Transition-metal-catalyzed C–C bond activation involving common organic functional groups is fundamental to access functionalized arenes.[3,4] In this vein, engaging native aldehyde functionality is intriguing as it involves successive C(sp^2)–H and C(sp^2)–C(sp^2) bond activation and materializes reactive organometallic species via CO extrusion for organic synthesis (Scheme 1b).[4] However, this strategy has primarily been documented with expensive Pd- and Rh-catalysts, and the efficacy of relatively cheap Ru(II)-catalysts has proven insufficient in many instances. Nonetheless, in 2009, Li *et al.* showcased $[Ru(COD)Cl_2]_n$ catalyzed decarbonylative addition of aromatic aldehyde to terminal alkynes to prepare olefins (scheme 1c).[5]

We envisaged that Ru(II)-catalyzed deformylative coupling of *ortho*-hydroxy aromatic aldehydes with readily prepared cyclic diazo compounds[6] could be a succinct strategy to access biaryldiol frameworks (Scheme 1d). We planned to explore bench-stable $[Ru(p\text{-cymene})Cl_2]_2$ cata-

lyst and anticipated a dual role for the hydroxyl group, facilitating the deformylation reaction through chelation to the Ru(II)-catalyst and serving as an integral component of the resulting biaryldiol frameworks. Initially, *ortho*-hydroxy aromatic aldehyde **1** will coordinate to Ru(II)-catalyst and then transform into the key ruthenacycle **A** via a formal deformylation event. Subsequent reaction with

Scheme 1. Biaryldiol Scaffolds and Deformylative Transition Metal Catalysis

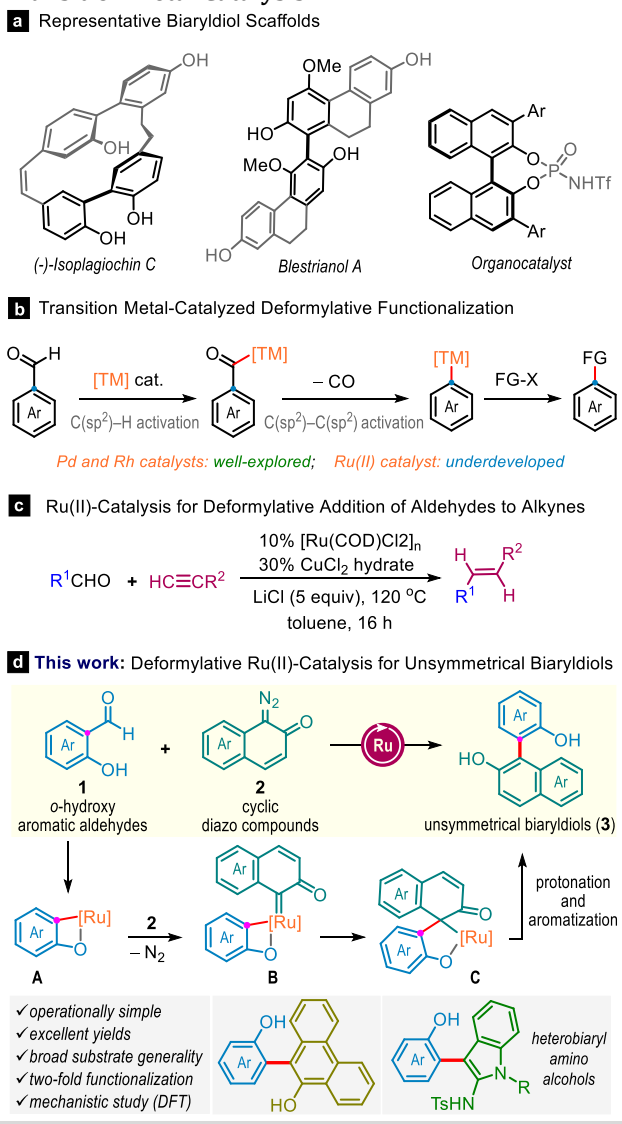

diazo compound **2** could lead to spirocyclic intermediate **C** through the intermediacy of metal-carbene species **B**, which upon protonation, would furnish unsymmetrical biaryldiol **3**. However, materialization of this blueprint must overcome several synthetic challenges. The sequence of bond-breaking and bond-forming steps should be in right order. Any alteration or premature termination would result in undesired byproducts. Also, direct insertion reaction of the free-hydroxyl group in starting material **1** as well as in product **3** with diazocompound **2** in the presence of metal-catalyst must be mitigated to preserve the efficacy of the reaction. Further, mild reaction conditions and the absence of external oxidant are significant to avoid the decomposition of substrates as well as biaryldiol product, albeit decarbonylative functionalization generally requires elevated reaction temperature due to the strong coordinating affinity of CO to metal catalyst.[4a]

Herein, we demonstrated the development of this reaction modality and reported the first example of Ru(II)-catalyzed deformylative biaryldiol synthesis. The reaction features a broader substrate's generality, excellent yields, regioselectivity, and efficacy in the presence of pharmacophore scaffolds. Synthesis of indole-containing biaryl amino alcohols was also accomplished through substrate design.[7] DFT studies were performed to comprehend the reaction mechanism.

RESULTS AND DISCUSSION

We commenced our investigation following the model reaction between 2-hydroxy-5-methylbenzaldehyde **1a** and diazonaphthoquinone **2a** in the presence of [Ru(*p*-cymene)Cl_2]$_2$ catalyst and NaOAc base (Table 1).

Table 1. Reaction Optimization[a]

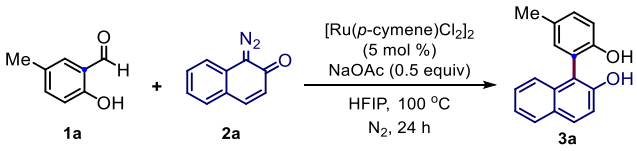

entry	deviation from standard conditions	yield (%)[b]
1	MeOH / TFE instead of HFIP	38 / 75
2	**none**	**96**
3	TFT / DCE / THF instead of HFIP	NR
4	CsOAc / KOAc instead of NaOAc	56 / 42
5	K_2CO_3 / Na_2CO_3 instead of NaOAc	NR
6	K_3PO_4 instead of NaOAc	NR
7	at 80 °C / 110 °C	61 / 82
8	NaOAc (1.0 equiv)	87
9	without NaOAc	NR
10	without [Ru(*p*-cymene)Cl_2]$_2$	NR
11	$Pd(OAc)_2$ or [Cp*$IrCl_2$]$_2$ instead of Ru(II)-catalyst	< 5%

[a]Reaction conditions: **1a** (0.3 mmol), **2a** (0.45 mmol), and HFIP (1.2 mL) under nitrogen atmosphere. [b]Isolated yields were provided.

To our delight, the desired deformylative coupling took place at 100 °C in methanol, albeit biaryldiol product **3a** was obtained in poor yield of 38% (Table 1, entry 1). When the reaction was tested in trifluoroethanol (TFE), a comparatively more acidic but less nucleophilic solvent, the yield was improved up to 75% (Table 1, entry 1). Further screening resulted in a clean reaction in hexafluoroisopropanol (HFIP) medium and the biaryldiol **3a** was isolated in 96% yield (entry 2), whereas aprotic solvents such as trifluorotoluene (TFT), 1,2-dichloroethane (DCE), and THF

proved unsuitable (entry 3). The reaction was sluggish for other acetate bases, for example, CsOAc and KOAc (entry 4) and completely inhibited in the presence of carbonates and phosphate bases (entries 5-6). Performing the reaction at lower (80 °C) or higher (110 °C) temperature gave inferior outcomes (entry 7). The loading of base was critical as yield reduced with the increased amount of NaOAc (1 equiv); on the other hand, the reaction completely shut down without it (entries 8-9). Control experiments showed that the Ru(II)-catalyst is highly significant for this deformylative coupling (entry 10). In contrast, renowned $Pd(OAc)_2$ and $[Cp^*IrCl_2]_2$ catalysts were ineffective in promoting the reaction (entry 11).

Scheme 2. Exploration of Substrate Scope

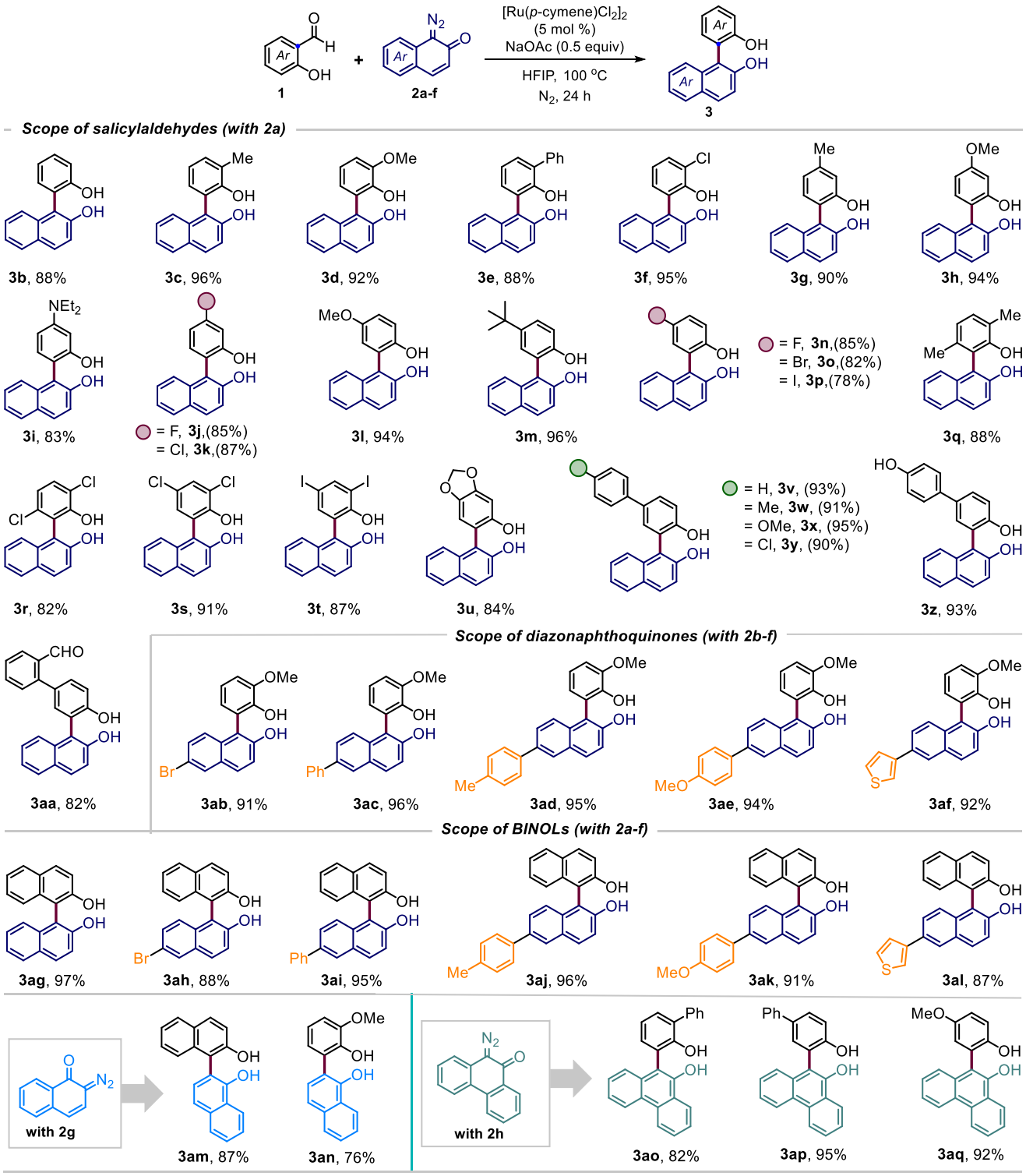

https://doi.org/10.26434/chemrxiv-2024-3j2r1 **ORCID:** https://orcid.org/0000-0001-9415-7137

Scheme 2. *Continued*

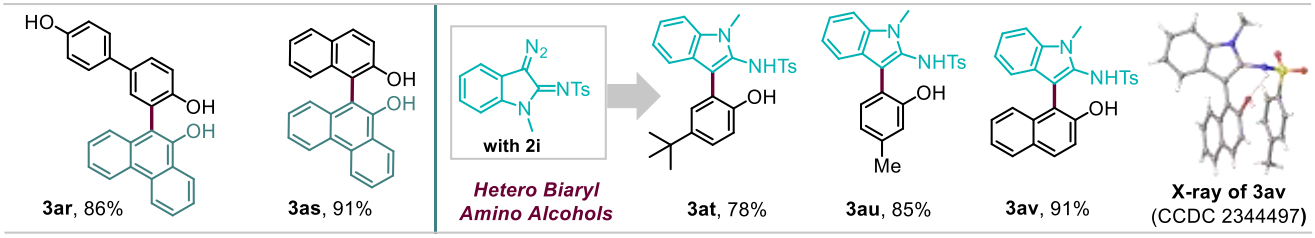

Reaction conditions: **1** (0.3 mmol), **2** (0.45 mmol), HFIP (1.2 mL) for 24 h under N_2 atmosphere. Isolated yields were provided.

With the optimization conditions in hand (Table 1, entry 2), the scope of this ruthenium catalyzed C–C activation reaction was explored (Scheme 2). The reaction was fertile across various structurally diverse *ortho*-hydroxy aromatic aldehydes. The parent salicylaldehyde (**3b**) along with alkyl (**3c**), alkoxy (**3d**), phenyl (**3e**), and chloro (**3f**) substitutions at the C3-position furnished the desired biaryldiols in excellent yields (88–96%). Similarly, aldehydes bearing a range of electron-donating as well as electron-withdrawing halogen functionalities at the C4- and C5-position effectively participated in this process to dispense **3g–3p** in uniformly very high yields. The sterically demanding *ortho*-hydroxy aromatic aldehydes having disubstitution at the C3- and C6-positions were also suitable, offering **3q** and **3r** in 88% and 82% yields, respectively. Other dihalogen-containing and 1,3-dioxolane-fused salicylaldehydes gave products **3s–3u** in excellent yields. Reactions of aldehyde substrates encompassing functionally enriched aryl motifs, endorsing extended conjugation, were also fruitful in producing **3v–3z** and **3aa** in 82%–95% yields. Notably, the formation of **3aa** took place via site-selective functionalization at the salicylaldehyde unit, suggesting the presence of both formyl and hydroxyl groups in the same aryl ring is important.

Next, we evaluated the reaction efficacy with substituted diazonaphthoquinones **2b–f** (Scheme 2). The synthetically modifiable bromo-containing diazonaphthoquinone produced **3ab** in 91% yield. Aryl (**3ac–3ae**) and heteroaryl (**3af**) substitutions in **2a** were also tolerable. Interestingly, the C–C activation-guided coupling with 2-hydroxy-1-naphthaldehyde was amenable, resulting in valuable symmetrical and unsymmetrical BINOL analogs (**3ag–3al**) in excellent yields.

To extend the scaffold diversity, we set out further exploration with various structurally distinct diazo compounds (Scheme 2). Under standard reaction conditions, examination of diazonaphthoquinone **2g**, a regioisomer of the diazo compound **2a**, was rewarding to afford **3am** and **3an** in 87% and 76% yields, respectively. The reaction with 9-diazo-10-oxophenanthrene **2h** also proceeded smoothly, and unsymmetrical biaryldiols **3ao–3as** were isolated in excellent yields (82%–95%). Gratifyingly, coupling was equally effective with indole-embedded diazo-imine **2i** to offer challenging heterobiaryl amino alcohols **3at–3av** in very high to excellent yields. The compound **3av** was crystallized, and the single-crystal *X*-ray analysis unequivocally confirmed the product structure and regioselectivity (Scheme 2).

Pleasingly, two-fold C–C activation was feasible when 4,4'-dihydroxy-3,3'-diformylbiphenyl **4** substrate was considered (Scheme 3). Coupling with diazoquinones **2a**, **2c**, **2g**, and **2h** offered valuable tetrahydroxy biaryl scaffolds **5a–5d** in 72%-90% yields. Two-fold C–C activation was also successful with indole-embedded diazo-imine **2i** and the desired heterobiaryl amino alcohol **5e** was isolated in good yield (Scheme 3).

Scheme 3. Demonstration of Two-fold C–C Activation.

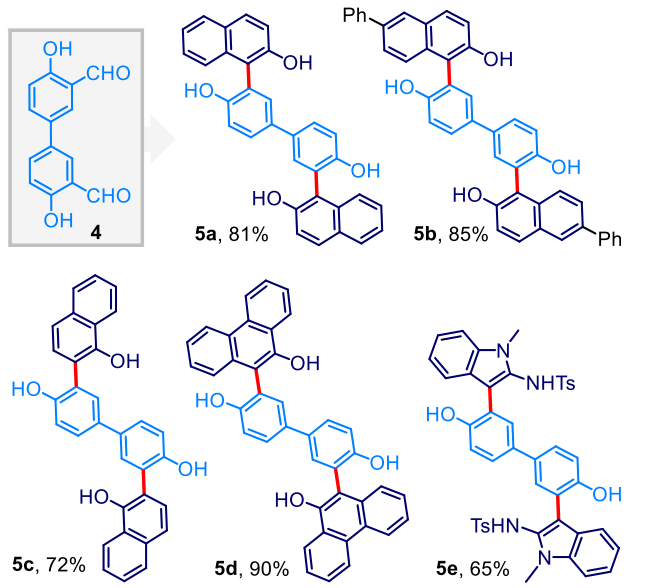

To expand the synthetic value further, we applied this Ru(II)-catalyzed deformylative C–C activation reaction for the late-stage functionalization of pharmaceuticals (Scheme 4). Under the standard reaction conditions, estrone-derived aldehyde **6a** was smoothly coupled with diazo compounds **2a**, **2h**, and **2i** to furnish biologically relevant diols **7aa–7ab** and amino alcohol **7ac** in high yields. Similarly, reactions with *L*-tyrosine derived aldehyde **6b** were fruitful and the desired tyrosine-embedded biaryl frameworks **7ba–7bc** were isolated in 69%–83% yields (Scheme 4).

Scheme 4. Late-stage Functionalization of Pharmacophore Scaffolds

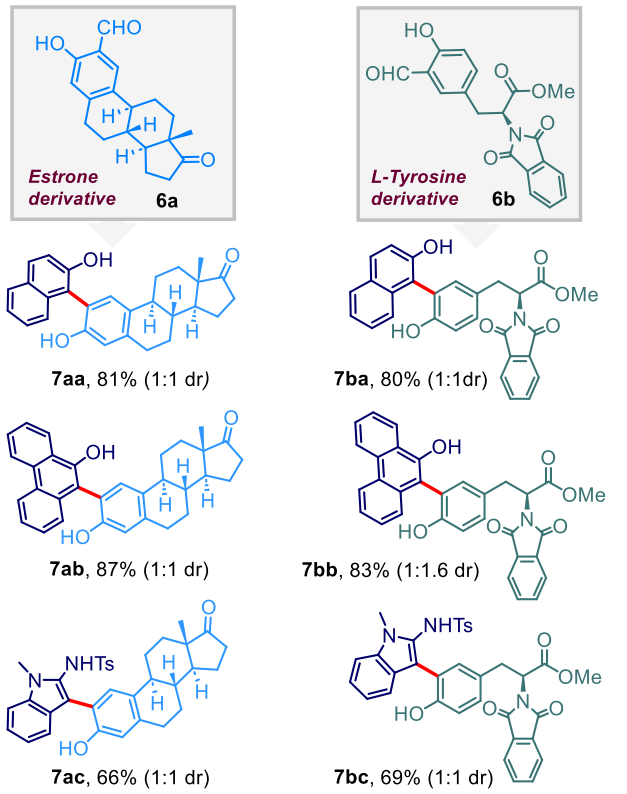

Of note, the efficiency of the small-scale reaction was comparable upon scale-up. From 3 mmol scale reactions, biaryldiols **3ag** and **3ai** were isolated in 93% and 91% yields, respectively (Scheme 5a). The biaryldiols were also readily converted to valuable π-conjugated polycyclic benzofurans **8ah–8ak** in high yields, showcasing synthetic utility (Scheme 5b).[8]

Scheme 5. Scale-up Reactions and Post-synthetic Manipulations

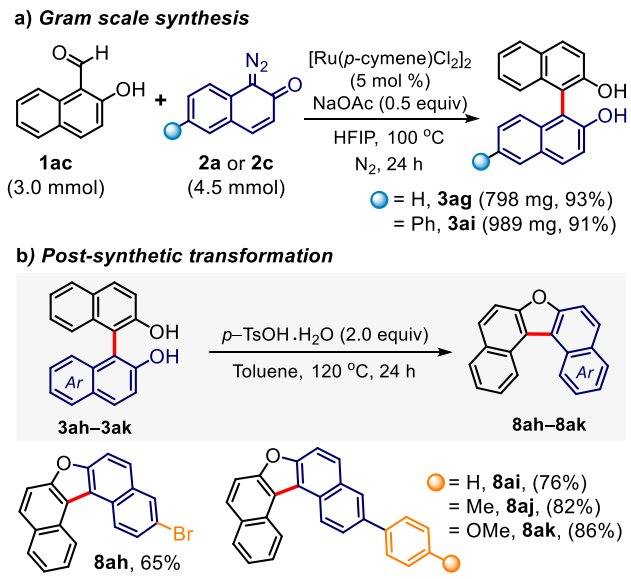

Scheme 6. Control Experiments

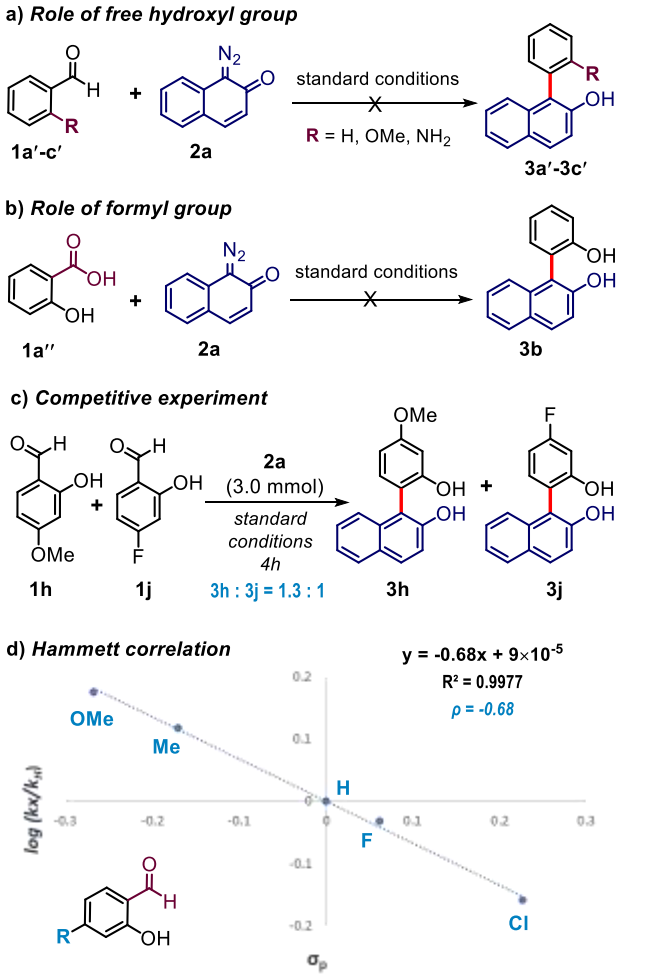

To shed light on the reaction modality, various control experiments were conducted (Scheme 6). The presence of an *ortho*-hydroxyl group in aromatic aldehyde substrate is very critical for the success of this protocol, and the reaction was unproductive in the absence of it or when it was replaced with methoxy or amine functionality (Scheme 6a). Execution of this strategy with salicylic acid **1a′** was also unfruitful, indicating this reaction proceeds exclusively through the involvement of the formyl group (Scheme 6b). A competition experiment between electronically different substrates revealed that the reaction with electron-rich methoxy-substituted aldehyde **1h** proceeds 1.3 times faster than the electron-deficient fluoro-substituted aldehyde **1j** (Scheme 6c). Also, we obtained the Hammett correlation with a negative ρ value (ρ = −0.68), implying the decrease of the electron density in the aromatic ring during the course of the reaction (Scheme 6d).

To gain deeper mechanistic insights, we conducted electronic structure calculations using density functional theory (DFT) (Scheme 7a). Initially, intermediate **INT2** forms through a formal ligand exchange reaction between the [Ru(*p*-cymene)(OAc)$_2$] complex **INT1** and the 2-hydroxybenzaldehyde substrate **1b**.

Scheme 7. DFT Calculation[a]

a) *Free energy profile for deformylative coupling towards biaryldiol*

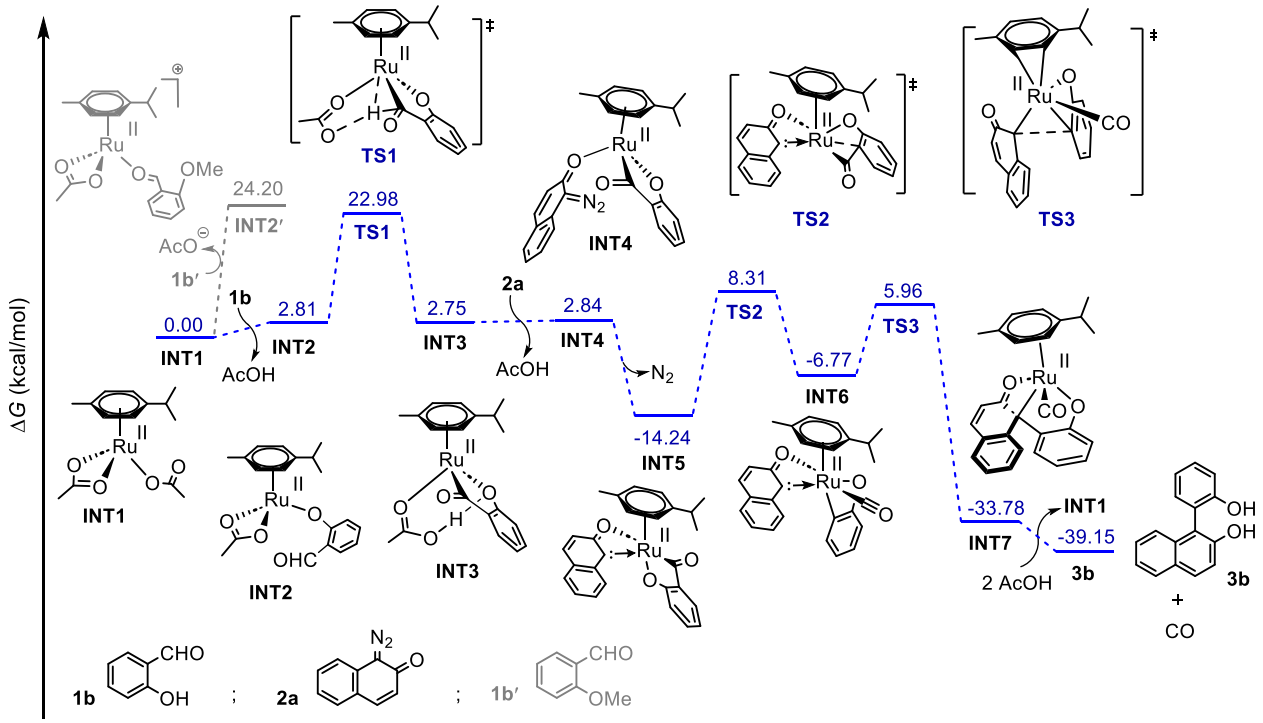

b) *Comparison of decarbonylation and without decarbonylation pathways*

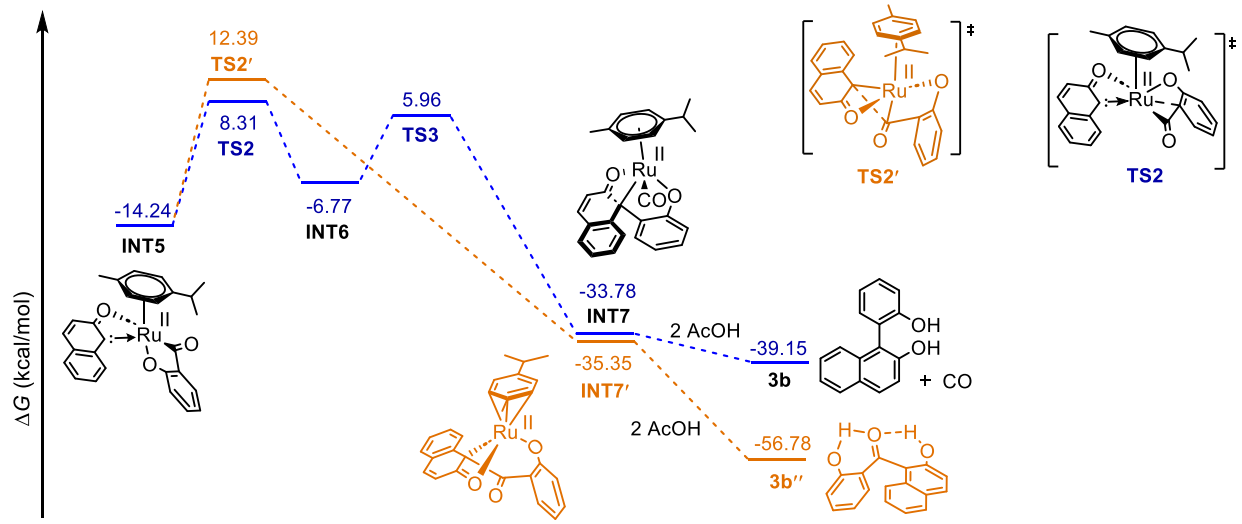

[a]All calculations were performed using M06L functional along with 6-31G(d,p) and SDD(ECP) as basis set for main group atoms and ruthenium, respectively. Implicit HFIP solvent conditions were mimicked employing self-consistent reaction field (SCRF) method SMD. Relative free energies are given in kcal/mol.

Investigation of a similar ligand exchange reaction with 2-methoxybenzaldehyde (**1b'**), where deprotonation of the phenolic hydroxyl group is not feasible, resulted in intermediate **INT2'**, which is disfavored by ~24 kcal/mol. This result is in line with our control experiment depicted in Scheme 6a. Next, the activation of the C–H bond of the formyl group generates the five-membered ruthenacycle **INT3** via **TS1**, with a barrier of approximately 23 kcal/mol. The diazo compound **2a** then coordinates to the ruthenium center, displacing AcOH to form **INT4**, which promptly transforms to **INT5** by extruding molecular nitrogen. Subsequent C–C(O) cleavage results in the formation of the four-membered ruthenacycle **INT6** via **TS2** with an activation barrier of 22.5 kcal/mol that is similar to the preceding C–H activation step (**INT2→INT3**). The migratory insertion step is highly exergonic, releasing 27.01 kcal/mol energy to

give **INT7** via **TS3**, with an activation barrier of 20.2 kcal/mol. Finally, upon protodemetalation, the 1,1-biaryldiol product **3b** is formed and active ruthenium catalyst is regenerated to continue the cycle. Overall, deformylation, rather than insertion, appears to be the likely rate-limiting process for this transformation.

Additionally, DFT studies suggest that direct C–C bond formation from **INT5**, prior to carbonyl expulsion, has a higher activation energy (Scheme 7b, **TS2**, 22.6 kcal/mol vs. **TS2'**, 26.6 kcal/mol). This provides a possible explanation for why decarbonylation is exclusively observed in our experiments, despite product **3b"** being ~ 17.6 kcal/mol more stable than the 1,1-biaryldiol product **3b** (Scheme 7b).

CONCLUSIONS

In conclusion, we have developed a cogent and diversified synthesis of challenging unsymmetrical 1,1′-biaryl-2,2′-diols by harnessing inexpensive Ru(II)-catalyzed regioselective coupling of *ortho*-hydroxy aromatic aldehydes with a variety of cyclic diazo compounds under mild conditions. The reaction capitalizes on the formal deformylative C–C activation and carbene insertion manifold and leverages a dual-role of the *ortho*-hydroxy aromatic aldehyde substrates to produce a wide spectrum of diversely functionalized biaryl diols in very high to excellent yields. Further substrate design allowed facile access to valuable heterobiaryl amino alcohols and enables challenging two-fold C–C activation *en route* to valuable tetrahydroxy bis-biaryls. The protocol is operationally simple, scalable, and also suitable for the site-selective modification of pharmaceutical agents. Comprehensive investigations, including DFT studies and control experiments, have provided insights into the underlying mechanism of the reaction, highlighting the energetically significant deformylation event over the carbene insertion step. Notably, our methodology represents a rare instance of C–C activation-guided Ru(II)-catalysis for producing high-value 1,1'-biaryl-2,2'-diol frameworks.

ASSOCIATED CONTENT

AUTHOR INFORMATION

Corresponding Authors

Prof. Soumya Ghosh, Tata Institute of Fundamental Research (TIFR), Hyderabad, Telangana 500046, India.
Email: soumya.ghosh@tifrh.res.in

Prof. Mahiuddin Baidya, Department of Chemistry, Indian Institute of Technology, Madras, Chennai-600036, India.
Email: mbaidya@iitm.ac.in

Supporting Information

Complete experimental details, characterization data for the prepared compounds, Cartesian coordinates of DFT optimized structures, and crystallographic data (CIF).

ACKNOWLEDGMENTS

M.B. gratefully acknowledges SERB, India (CRG/2023/001052) for the financial support. S.G. acknowledges support of the Department of Atomic Energy, GOI (project identification no. RTI 4007). C. K. G. thanks UGC for the SRF and S. M. acknowledges IIT Madras for providing the HTRA fellowship. M.B. appreciates affiliation with the National Center for Catalysis Research (NCCR) and Center for Chiral Technology of IIT Madras. We also thank the Department of Chemistry and SAIF, IIT Madras for the instrumental facilities.

REFERENCES

1. (a) For a book, see: Cepanec, I. *Synthesis of Biaryls*, Elsevier Science, **2004**, *DOI: 10.1016/B978-0-08-044412-3.X5000-3*. For selected reviews: (b) Bringmann, G.; Walter, R.; Weirich, R. The Directed Synthesis of Biaryl Compounds: Modern Concepts and Strategies. *Angew. Chem., Int. Ed.* **1990**, *29*, 977–991. (c) Pu, L. 1,1′-Binaphthyl Dimers, Oligomers, and Polymers: Molecular Recognition, Asymmetric Catalysis, and New Materials. *Chem. Rev.* **1998**, *98*, 2405–2494. (d) Telfer, S. G.; Kuroda, R. 1,1′-Binaphthyl-2,2′-Diol and 2,2′-Diamino-1,1′ -Binaphthyl: Versatile Frameworks for Chiral Ligands in Coordination and Metallosupramolecular Chemistry. *Coord. Chem. Rev.* **2003**, *242*, 33–46. (e) Chen, Y.; Yekta, S.; Yudin, A. K. Modified BINOL Ligands in Asymmetric Catalysis. *Chem. Rev.* **2003**, *103*, 3155–3211. (f) Bringmann, G.; Mortimer, A. J. P.; Keller, P. A.; Gresser, M. J.; Garner, J.; Breuning, M. Atroposelective Synthesis of Axially Chiral Biaryl Compounds. *Angew. Chem., Int. Ed.* **2005**, *44*, 5384–5427. (g) Shibasaki, M.; Matsunaga, S. Design and Application of Linked-BINOL Chiral Ligands in Bifunctional Asymmetric Catalysis. *Chem. Soc. Rev.* **2006**, *35*, 269–279. (h) Kozlowski, M. C.; Morgan, B. J.; Linton, E. C. Total Synthesis of Chiral Biaryl Natural Products by Asymmetric Biaryl Coupling. *Chem. Soc. Rev.* **2009**, *38*, 3193–3207. (i) Simonetti, M.; Cannas, D. M.; Larrosa, I. Biaryl Synthesis via C–H Bond Activation: Strategies and Methods. *Adv. Organomet. Chem.* **2017**, *67*, 299–399. (j) Parmar, D.; Sugiono, E.; Raja, S.; Rueping, M. Complete Field Guide to Asymmetric BINOL-Phosphate Derived Brønsted Acid and Metal Catalysis: History and Classification by Mode of Activation; Brønsted Acidity, Hydrogen Bonding, Ion Pairing, and Metal Phosphates. *Chem. Rev.* **2014**, *114*, 9047–9153. (k) Liao, G.; Zhou, T.; Yao, Q. J.; Shi, B. F. Recent Advances in the Synthesis of Axially Chiral Biaryls: Via Transition Metal-Catalysed Asymmetric C-H Functionalization. *Chem. Commun.* **2019**, *55*, 8514–8523. (l) Cheng, J. K.; Xiang, S. H.; Li, S.; Ye, L.; Tan, B. Recent Advances in Catalytic Asymmetric Construction of Atropisomers. *Chem. Rev.* **2021**, *121*, 4805–4902. (m) Yue, Q.; Liu, B.; Liao, G.; Shi, B. F. Binaphthyl Scaffold: A Class of Versatile Structure in Asymmetric C-H Functionalization. *ACS Catal.* **2022**, *12*, 9359–9396.

2. (a) Bringmann, G.; Gulder, T.; Gulder, T. A. M.; Breuning, M. Atroposelective Total Synthesis of Axially Chiral Biaryl Natural Products. *Chem. Rev.* **2011**, *111*, 563–639. (b) Wang, Y.; Tan, B. Construction of Axially Chiral Compounds via Asymmetric Organocatalysis. *Acc. Chem. Res.* **2018**, *51*, 534–547. For selected examples see: (c) Kamitanaka, T.; Morimoto, K.; Tsuboshima, K.; Koseki, D.; Takamuro, H.; Dohi, T.; Kita, Y. Efficient Coupling Reaction of Quinone Monoacetal with Phenols Leading to Phenol Biaryls. *Angew. Chem., Int. Ed.* **2016**, *55*, 15535–15538. (d) Gao, J.; Wang, P.; Shen, A.; Yang, X.; Cen, S.; Zhang, Z. Axially Chiral Copper Catalyst for Asymmetric Synthesis of Valuable Diversely Substituted BINOLs. *ACS Catal.* **2024**, *14*, 5621–5629.

3. For selected reviews, see: (a) Jun, C. Transition Metal-Catalyzed Carbon–Carbon Bond Activation. *Chem. Soc. Rev.* **2004**, *33*, 610–618. (b) Ruhland, K. Transition-Metal-Mediated Cleavage and Activation of C–C Single Bonds. *Eur. J. Org. Chem.* **2012**, 2683–2706. (c) Chen, F.; Wang, T.; Jiao, N. Recent Advances in Transition-Metal-Catalyzed Functionalization of Unstrained Carbon-Carbon Bonds. *Chem. Rev.* **2014**, *114*, 8613–8661. (d) Dermenci, A.; Coe, J. W.; Dong, G. Direct Activation of Relatively Unstrained Carbon-Carbon Bonds in Homogeneous Systems. *Org. Chem. Front.* **2014**, *1*, 567–581. (e) Souillart, L.; Cramer, N. Catalytic C-C Bond Activations via Oxidative Addition to Transition Metals. *Chem. Rev.* **2015**, *115*, 9410–9464. (f) Marek, I.; Masarwa, A.; Delaye, P. O.; Leibeling, M. Selective Carbon-Carbon Bond Cleavage for the Stereoselective Synthesis of Acyclic Systems. *Angew. Chem., Int. Ed.* **2015**, *54*, 414–429. (g) Lutz, M. D. R.; Morandi, B. Metal-Catalyzed Carbon-Carbon

Bond Cleavage of Unstrained Alcohols. *Chem. Rev.* **2021**, *121*, 300–326. (h) Nanda, T.; Fastheem, M.; Linda, A.; Pati, B. V.; Banjare, S. K.; Biswal, P.; Ravikumar, P. C. Recent Advancement in Palladium-Catalyzed C-C Bond Activation of Strained Ring Systems: Three-and Four-Membered Carbocycles as Prominent C3/C4 Building Blocks. *ACS Catal.* **2022**, *12*, 13247–13281. (i) Song, F.; Wang, B.; Shi, Z. J. Transition-Metal-Catalyzed C–C Bond Formation from C–C Activation. *Acc. Chem. Res.* **2023**, *56*, 2867–2886. For selected papers, see: (j) Gooßen, L. J.; Deng, G.; Levy, L. M. Synthesis of Biaryls via Catalytic Decarboxylative Coupling. *Science* **2006**, *313*, 662. (k) Kaishap, P. P.; Duarah, G.; Sarma, B.; Chetia, D.; Gogoi, S. Ruthenium(II)-Catalyzed Synthesis of Spirobenzofuranones by a Decarbonylative Annulation Reaction. *Angew. Chem., Int. Ed.* **2018**, *57*, 456–460. (l) Zhou, T.; Ji, C. L.; Hong, X.; Szostak, M. Palladium-Catalyzed Decarbonylative Suzuki-Miyaura Cross-Coupling of Amides by Carbon-Nitrogen Bond Activation. *Chem. Sci.* **2019**, *10*, 9865–9871. (m) Liu, C.; Ji, C. L.; Zhou, T.; Hong, X.; Szostak, M. Bimetallic Cooperative Catalysis for Decarbonylative Heteroarylation of Carboxylic Acids via C–O/C–H Coupling. *Angew. Chem., Int. Ed.* **2021**, *60*, 10690–10699. (n) Yang, S.; Yu, X.; Szostak, M. Divergent Acyl and Decarbonylative Liebeskind-Srogl Cross-Coupling of Thioesters by Cu-Cofactor and Pd-NHC (NHC = N–Heterocyclic Carbene) Catalysis. *ACS Catal.* **2023**, *13*, 1848–1855. (o) Yu, C.; Zhang, Z.; Dong, G. Split Cross-Coupling via Rh-Catalysed Activation of Unstrained Aryl–Aryl Bonds. *Nat. Catal.* **2024**, *DOI: 10.1038/s41929-024-01120-9*.

4. For selected reviews, see: (a) Lu, H.; Yu, T. Y.; Xu, P. F.; Wei, H. Selective Decarbonylation via Transition-Metal-Catalyzed Carbon-Carbon Bond Cleavage. *Chem. Rev.* **2021**, *121*, 365–411. (b) Saikia, P.; Gogoi, S. Recent Advances in Decarbonylative Annulation Reactions. *Org. Biomol. Chem.* **2021**, *19*, 8853–8873. For selective examples see: (c) Shuai, Q.; Yang, L.; Guo, X.; Baslě, O.; Li, C. J. Rhodium-Catalyzed Oxidative C–H Arylation of 2-Arylpyridine Derivatives via Decarbonylation of Aromatic Aldehydes. *J. Am. Chem. Soc.* **2010**, *132*, 12212–12213. (d) Modak, A.; Deb, A.; Patra, T.; Rana, S.; Maity, S.; Maiti, D. A General and Efficient Aldehyde Decarbonylation Reaction by Using a Palladium Catalyst. *Chem. Commun.,* **2012**, *48*, 4253–4255. (e) Sun, P.; Gao, S.; Yang, C.; Guo, S.; Lin, A.; Yao, H. Controllable Rh(III)-Catalyzed Annulation between Salicylaldehydes and Diazo Compounds: Divergent Synthesis of Chromones and Benzofurans. *Org. Lett.* **2016**, *18*, 6464–6467. (f) Rao, M. L. N.; Ramakrishna, B. S. Rh-Catalyzed Deformylative Coupling of Salicylaldehydes with Acrylates and Acrylamides. *J. Org. Chem.* **2019**, *84*, 5677–5683. (g) Guo, L.; Srimontree, W.; Zhu, C.; Maity, B.; Liu, X.; Cavallo, L.; Rueping, M. Nickel-Catalyzed Suzuki–Miyaura Cross-Couplings of Aldehydes. *Nat. Commun.* **2019**, *10*, 1957. (h) Li, X.; Shen, Y.; Zhang, G.; Zheng, X.; Zhao, Q.; Song, Z. Ru(II)-Catalyzed Decarbonylative Alkylation and Annulations of Benzaldehydes with Iodonium Ylides under Chelation Assistance. *Org. Lett.* **2022**, *24*, 5281–5286.

5. (a) Guo, X.; Wang, J.; Li, C. J. An Olefination via Ruthenium-Catalyzed Decarbonylative Addition of Aldehydes to Terminal Alkynes. *J. Am. Chem. Soc.* **2009**, *131*, 15092–15093. (b) Guo, X.; Wang, J.; Li, C. J. Ru-Catalyzed Decarbonylative Addition of Aliphatic Aldehydes to Terminal Alkynes. *Org. Lett.* **2010**, *12*, 3176–3178.

6. (a) Nawrat, C. C.; Moody, C. J. Natural Products Containing a Diazo Group. *Nat. Prod. Rep.* **2011**, *28*, 1426–1444. (b) Doyle, M. P.; Duffy, R.; Ratnikov, M.; Zhou, L. Catalytic Carbene Insertion into C–H Bonds. *Chem. Rev.* **2010**, *110*, 704–724. (c) Ford, A.; Miel, H.; Ring, A.; Slattery, C. N.; Maguire, A.R.; McKervey, M. A. Modern Organic Synthesis with *α*-Diazocarbonyl Compounds. *Chem. Rev.* **2015**, *115*, 9981–10080.

7. (a) Ding, K.; Li, X.; Ji, B.; Guo, H.; Kitamura, M. Ten years of research on NOBIN chemistry. *Curr. Org. Synth.* **2005**, *2*, 499–545. (b) Patel, D. C.; Breitbach, Z. S.; Woods, R. M.; Lim, Y.; Wang, A.; Jr, F. W. F.; Armstrong, D. W. Gram Scale Conversion of R-BINAM to R-NOBIN. *J. Org. Chem.* **2016**, *81*, 1295–1299. (c) Chen, Y. H.; Qi, L. W.; Fang, F.; Tan, B. Organocatalytic Atroposelective Arylation of 2-Naphthylamines as a Practical Approach to Axially Chiral Biaryl Amino Alcohols. *Angew. Chem., Int. Ed.* **2017**, *56*, 16308–16312. (d) Yang, G.; Guo, D.; Meng, D.; Wang, J. NHC–Catalyzed Atropoenantioselective Synthesis of Axially Chiral Biaryl Amino Alcohols via a Cooperative Strategy. *Nat. Commun.* **2019**, *10*, 3062.

8. Shen, Y.; Chen, C.-F. Helicenes: Synthesis and Applications. *Chem. Rev.* **2012**, *112*, 1463–1535.